Journal Pre-proof

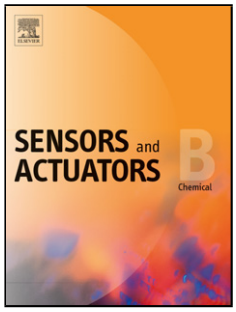

Chemiresistive detection of silver ions in aqueous media

Johnson Dalmieda (Methodology) (Investigation) (Writing - original draft), Ana Zubiarrain-Laserna (Methodology) (Investigation) (Writing - original draft), Devanjith Ganepola (Investigation), P. Ravi Selvaganapathy (Conceptualization) (Writing - review and editing), Peter Kruse (Supervision) (Conceptualization) (Methodology) (Writing - review and editing)

PII: S0925-4005(20)31370-8

DOI: https://doi.org/10.1016/j.snb.2020.129023

Reference: SNB 129023

To appear in: *Sensors and Actuators: B. Chemical*

Received Date: 11 May 2020

Revised Date: 28 September 2020

Accepted Date: 8 October 2020

Please cite this article as: { doi: https://doi.org/

Chemiresistive detection of silver ions in aqueous media

Johnson Dalmieda[1], Ana Zubiarrain-Laserna[1], Devanjith Ganepola[1], P. Ravi Selvaganapathy[2], Peter Kruse[1]*

[1]*Department of Chemistry and Chemical Biology, McMaster University, Hamilton L8S 4M1, Canada*

[2]*Department of Mechanical Engineering, McMaster University, Hamilton L8S 4M1, Canada*

*Author to whom correspondence should be addressed, email: pkruse@mcmaster.ca

Keywords: Water Quality; Heavy Metal Sensing; Silver; Cation Sensing; Graphene; Chemiresistive Sensor

Highlights:

- Chemiresistive sensors can be fabricated from percolation networks of few-layer graphene (FLG) flakes.
- Functionalization with suitable ligand molecules (e.g. bathocuproine) can achieve selective sensor response to dissolved Ag^+ ions in the 3 ppb to 1 ppm range.
- Sensors are robust and reusable, can be reset at pH3 due to a shift in the complexation equilibrium.
- The sensor response was tested in an environmental sample (river water) and found to correlate well with ICP-MS data.

Abstract

Silver is used as a water disinfectant in hospital settings as well as in purifiers for potable water. Although there are no strict regulations on the concentration of silver in water, adverse effects such as argyria and respiratory tract irritation have been correlated to excess silver consumption. Based on this, the levels of silver in water are recommended to be maintained below 100 ppb to ensure safety for human consumption. In this work, we present a silver sensor for use in aqueous media that utilizes bathocuproine, a silver selective chromophore, adsorbed onto few-layer graphene (FLG) flake networks for the chemiresistive detection of silver. Complexation of silver to bathocuproine modulates the conductivity of the FLG film, which can be probed by applying a small voltage bias. The decrease in resistance of the film correlates with the concentration of silver in solution between 3 ppb and 1 ppm. Exposing the sensor to a lower pH resets the sensor, allowing it to be reused and reset multiple times. This sensor demonstrates a new pathway to chemiresistive cation sensing using known selective complexing agents adsorbed onto graphitic thin films. This concept can be expanded to the detection of other relevant analytes in domestic, industrial and environmental water sources.

1. Introduction

Metallic silver is commonly used in water filters to reduce the growth of biofilms within the filter itself. Silver (I) ions are used as an effective disinfectant for potable water, giving a $\log_{10}$ reduction for *L. pneumophilia*, *P. aeruginosa*, and *E. coli* of 2.4, 4, and 7, respectively.[1] Hospitals use copper-silver ionization for *Legionella* control in their hot water systems.[2] On the other hand, silver is not an essential metal for humans, and exposure should be limited to avoid adverse effect such as argyria[3] and respiratory tract irritation.[4,5] In the environment, high concentrations of silver salts can pose a threat to various aquatic organisms. The median lethal concentration (LC_{50}) is 58 ppb for fish and 4.8 ppm for nematodes. Crustaceans are the most sensitive however, with an LC_{50} of 0.85 ppb.[6] Currently there are no guidelines for silver ions in drinking water, and the World Health Organization (WHO) has set a health advisory (not a guideline value) of 100 ppb. The only country with a Maximum Allowable Content (MAC) is Germany, whose drinking water regulations (Trinkwasserverordnung) prescribe a MAC of 80 ppb.[7]

Several methods are currently available for the quantification of silver (I) ions in water. Lee et. al. functionalized a quartz crystal microbalance (QCM) with a suitable oligonucleotide for the detection of silver (I) in aqueous solution, resulting in a limit of detection (LOD) of 100 pM (0.01 ppb) and a limit of quantification (LOQ) of 1 nM (0.1 ppb).[8] Colorimetric approaches to silver (I) detection include use of dyes such as a water-soluble organometallic polyelectrolyte (LOD=54 ppb)[9], Tween-20 functionalized gold nanoparticles (LOD=43 ppb)[10], a Rhodamine B derivative (LOD=14 ppb)[11], and an anthracene derivative.[12] Electrochemical methods include ion selective electrodes (ISE) utilizing copper (II) ionophore (I) (LOD=65 ppt)[13] or calixarene derivatives (LOD=10 ppm)[14], as well as anodic stripping voltammetry (ASV), such as one developed by Schildkraut et. al., which utilized a carbon paste electrode to determine silver (I) in surface water (LOD=0.2 ppb)[15], and one developed by Zejli et. al., which used a polythiophene-functionalized platinum electrode (LOD=60 ppb).[16] For ultra trace detection of silver (I) in water, standard methods exist such as inductively coupled plasma-mass spectrometry (ICP-MS) (EPA method 200.8), inductively coupled plasma-absorption emission spectroscopy (ICP-AES) (EPA method 200.7), and flame atomic absorption spectroscopy (FAAS) (EPA method 7000B) (CASRN 7440-22-4).

Although these methods, as well as many more[17,18], have been used for silver (I) detection, there are various limitations that need to be addressed. QCM sensors are not

reusable, as they fail to reproduce their frequency shifts upon repeated exposure to silver (I). Colorimetric methods suffer from matrix effects in real samples that may hinder the colorimetric response or quench the fluorescence of the sensor molecules. ISE's and ASV require reference electrodes, which are easily damaged and require frequent recalibration and maintenance. The standard laboratory methods such as FAAS, ICP-MS, and ICP-AES, although highly sensitive and selective, require elaborate instrumentation and sample workup, effectively ruling out *in situ* measurements.

Here we propose the use of chemiresistive sensors[19] functionalized with a silver (I) ion selective ligand to detect silver (I) ions in aqueous media with sufficient sensitivity, specificity, and robustness. Chemiresistive sensors are based on modulating the electronic structure of the sensor films itself, obliviating the need for counter or reference electrodes. In our device, a percolation network of exfoliated few-layer graphene (FLG) flakes is connected to two copper contacts at either end and exposed to the silver ions such that only the FLG and not the contacts interact with the ions.[20] FLG is a semimetal with a high in-plane conductivity that is easily modulated by doping, a property crucial for signal transduction in the proposed sensors.[21] For applications in aqueous environments it is further important that FLG's basal plane is chemically inert, although it can be non-covalent functionalized through adsorption of aromatic molecules. Adsorption of these ion selective molecules does not destroy the electronic properties of FLG, but provides a handle for their modulation.[21] To functionalize the FLG, silver (I)-specific ligands, such as bathocuproine, can be adsorbed onto the film and interact with it electronically, imparting selectivity while preventing interactions with interfering ions.[22,23] Bathocuproine will add electron density to the FLG, effectively n-doping it. As silver ions bind to the bathocuproine on the FLG surface, changes in the energy levels of bathocuproine occur. This will cause a decrease in the resistance of the film. As the analyte concentration increases, so do the amount of complexed silver (I) ions, and the magnitude of the resistance change. We have previously demonstrated this principle to detect free chlorine in aqueous media using oligoanilines adsorbed onto carbon nanotubes or graphitic films.[24,25] The linear range for these sensor devices was from 60 ppb to 60 ppm, providing sufficient sensitivity for drinking water applications.[26] The FLG films with π-stacked selective molecules in these sensors are more chemically stable in real sample environments than films rich in surface defects needed for covalent bonding of the receptor molecules, as is common in other chemiresistive sensor designs.[27] This is also the first use of bathocuproine for reagentless silver (I) detection unlike the previously reported case of

copper (I) sensing, which requires the use of reducing agents.[28] The development of an aqueous silver (I) sensor is a departure from the redox-based response exhibited by the free chlorine sensor[24-26] to a complexometric based response, which can be used as a template for detection of various other metal cations.

2. Experimental

2.1. Materials

FLG was prepared from natural graphite powder (-200 mesh, 99.9999% trace metals basis, Alfa Aesar). 96% bathocuproine, 98% neocuproine, silver (I) nitrate, iron (II) chloride tetrahydrate, sodium phosphate monobasic monohydrate, chromium (III) chloride, aluminum (III) sulfate, cobalt (II) chloride, cadmium (II) chloride, zinc (II) chloride, copper (II) chloride, magnesium chloride hexahydrate, and calcium chloride dihydrate were purchased from Sigma Aldrich. Sodium sulphate, sodium chloride, sodium hydroxide, and sodium nitrate were purchased from Caledon. Potassium chloride and sodium bicarbonate were purchased from EMD Millipore. Ultrapure water (18.2 MΩ·cm) was obtained from a Millipore Simplicity UV water purifier unit. 1 M nitric acid was prepared by diluting 68% nitric acid (ACS reagent grade) with purified water. All organic solvents used were HPLC grade.

Standard solutions for the salts were prepared by dissolving the appropriate mass into 100 mL of purified water. The bathocuproine solution was prepared by dissolving the ligand into 30 mL of either methanol or acetonitrile until the solution is saturated. Since bathocuproine dissolves at a slower rate in acetonitrile, the solution was left in the dark overnight to dissolve.

Sensor devices were fabricated using twin frosted glass slides (purchased from VWR), freshly prepared exfoliated graphite, a 9B pencil, ¼" wide EMI Copper Foil Shielding Tape (3M #1181), and Sylgard 184 (Dow Chemical; silicone elastomer base was mixed with the curing agent in a 10:1 ratio).

2.2. Spectroscopic Characterization

UV-Vis spectra were obtained by mixing 2 mL of 5.0×10^{-5} M bathocuproine in acetonitrile with 5 mL of a 100 ppm solution of silver (I) nitrate in purified water. The solution was then

transferred to a quartz cuvette, and analysed using an Orion Aquamate 8000 spectrophotometer over a range of 200-500 nm.

Raman spectra of drop cast FLG films were recorded on a Renishaw inVia Raman spectrometer using a 514 nm laser and a 50× objective at 10% power with 3 accumulations over 30 seconds each.

Bathocuproine powder, a bathocuproine sample reacted with silver nitrate (as described for UV-Vis spectroscopy, then rinsed and dried), and a set of sensors underwent analysis by X-ray photoelectron spectroscopy (XPS) in order to confirm the functionalization of the films and to gain more insight into the sensing mechanism. The samples were analyzed using a Kratos AXIS Ultra X-ray photoelectron spectrometer. XPS survey spectra were obtained from an area of approximately 300 x 700 μm using a pass energy of 160 eV. XPS high resolution spectra were obtained from an area of approximately 300 x 700 μm using a pass energy of 20 eV. The devices sent for analysis were exposed to the same sequence of solutions. However, they were removed from the solutions at different stages. All devices were rinsed with ultrapure water at the end and they were stored under an inert nitrogen atmosphere until the time of analysis. All spectra were charge corrected to the C 1s binding energy of 284.5 eV for C=C.

2.3. Synthesis of exfoliated FLG

Exfoliated FLG flakes were prepared using a literature procedure.[29] 40 mg graphite was added to 15 g of 30% (w/w) isopropanol:water mixture in a 20 mL capped glass vial and sonicated in a bath sonicator (Elmasonic P30H Ultrasonic Cleaner) for six hours at 80 kHz (100% power) and 30 °C using the sweep setting.

The suspended FLG flakes were then centrifuged for 5 minutes at a relative centrifugal force (RCF) of 14100 × g (14500 rpm) in an Eppendorf MiniSpin plus centrifuge to separate the bulk unexfoliated graphite. The supernatant (with the exfoliated FLG) was retained, and re-centrifuged for 15 minutes at 14100 × g. The supernatant of the second centrifugation step (containing smaller, defect-rich graphene flakes) was discarded and the precipitate retained for sensor fabrication.

2.4. Sensor fabrication

Figure 1a shows an exploded view of the different components that make up a sensor. First, the glass slides were cleaned with methanol (Figure 2a) and two pencil graphite patches were drawn using a 9B pencil on opposite sides of the frosted side in order to decrease the contact resistance between the FLG films and the copper tape (Figure 2b). Then, the precipitate of exfoliated FLG was re-suspended in an isopropanol-water mixture and drop casted until a resistance of 10 – 20 kΩ was achieved (overall film size 21 × 18 mm: bare graphite 8 × 18 mm, pencil reinforcements 6.5 × 18 mm). The drop casting was performed on a hotplate at 100 °C to accelerate solvent evaporation (Figure 2c). Next, two adhesive copper tape strips were attached over the pencil contact reinforcements from end to end of the glass slide (Figure 2d). The sensors were packaged by masking the copper contacts with a thin layer of silicone elastomer. In order to prevent the elastomer from spreading over the FLG film, it was let to partially cure (approx. 6 hours at room temperature) so as to acquire a thicker consistency prior to application. The sensors were placed on a hotplate at 60 °C until the elastomer was completely cured (Figure 2e). A picture of a finished sensor is shown in Figure 1b. Images of the deposited FLG films were obtained with FESEM (JEOL JSM-7000F, Figures 1c and 1d), which show a network of FLG platelets arranged parallel to the glass slide. Raman spectroscopy was also used to study the quality of the FLG films (Figure 1e). The spectrum shows peaks characteristic of graphitic materials (namely the G, 2D and D + D'' bands). The absence of a shoulder in the 2D band suggests that the films consist of few layer graphene and not graphite, for which it should split into $2D_1$ and $2D_2$ components.[30] Finally, the D, D' and D + D' bands indicate that defects have been introduced in the flakes during processing. Some of these defects are related to the size of the platelets (i.e. edge defects).[31]

2.5. Sensor Characterization

An eDAQ EPU452 Quad Multi-Function isoPod with USB (purchased from eDAQ Inc) was used for data collection and was set to a polarization of 10 mV over a current range of 2000 nA. The sensors were run using the "Biosensor" configuration. A pH probe and a conductivity probe were also purchased from eDAQ Inc as part of an ER7006 Multisensor Kit. The pH probe was calibrated using two buffer solutions with pH 4 and pH 7 at 25 °C. The conductivity probe was calibrated using a 0.1 M KOH solution with a cell constant of 0.1 cm^{-1}. The eDAQ was connected to a computer via a USB serial controller for data acquisition and processing.

For the calibration experiment, four sensors were run in parallel. The sensors were first dipped in either methanol or acetonitrile in a glass jar for 5 minutes to wet the FLG surface. The sensors were then removed from the solvent, and three of the sensors were dipped into a solution of bathocuproine in either methanol or acetonitrile (the same solvent as used for wetting) for 3 hours to functionalize the FLG surface. The fourth sensor was placed back into the same solvent used for wetting and was used as a blank for control. After 3 hours, the sensors are removed from their respective solutions, and dried with a heat gun (pointed at the backside of the sensor). The sensors were then placed into separate glass jars filled with 50 mL of purified water and a stir bar. Each sensor was oriented facing the stir bar, with the sensor and the stir bar on opposite sides of the glass jar. The water was stirred, and the sensors were left overnight for 18-24 hours to equilibrate. Once equilibrated, appropriate amounts of the 100 ppm stock silver nitrate solution were added such that the Ag^+ ion concentration of the solution in the glass jars was 3 ppb. This was left for 1 hour, during which the current increased, and equilibrated after ~15 minutes. The same was done for 10 ppb, 30 ppb, 100 ppb, 300 ppb, and 1 ppm of Ag^+. To reset the sensors and return them to the 0 ppm baseline, the sensors were removed from the Ag^+ ion containing solution, placed into four jars with 30 mL of HNO_3 solution diluted from the 1M stock solution to a pH of 3, and left for one hour. The sensors were then removed from the pH 3 solution, rinsed with purified water, and placed into 50 mL of stirring purified water in glass jars for 18-24 hours (overnight) to equilibrate once more.

For the interference experiments, six sensors (four functionalized, two blank), as well as a pH probe and a conductivity probe were placed into a 1 L Pyrex bowl filled with 500 mL of stirring purified water and left overnight for 18-24 hours to equilibrate. The stir bar was placed at the centre of the bowl, with the sensors surrounding the perimeter of the bowl facing towards the centre. To test the pH response, a 1 M NaOH solution was used to adjust the pH to 10. Once the pH was set to 10, the sensors were left to run for one hour. The pH was then lowered to 9 using 1 M HNO_3 and was once again left for one hour. This was done for each pH value down to a pH of 3. To test for interferences, the purified water was treated with 1 M HNO_3 and sodium bicarbonate solution to adjust the pH and conductivity to 6.7 and 31 μS/cm, respectively (based on levels typically found in surface waters, such as Duchesnay Creek[32]). A stock solution of the interfering ion was then pipetted into the Pyrex bowl until the desired concentration was achieved. This was left for 20 minutes, after which the pH was dropped to 3 using 1 M HNO_3 to reset the sensors. The sensors were left to reset for 20

minutes, and then removed from the pH 3 solution. This was replaced by a fresh solution of stirring purified water with the pH and conductivity adjusted using 1 M HNO_3 and sodium bicarbonate and left for 20 minutes before adding the next interfering ion.

3. Results and Discussion

3.1. Sensing principle

The sensing principle for this sensor is based on the formation of a complex between bathocuproine (Figure 2 inset) and silver (I). Bathocuproine has been used as an exciton blocking layer in organic photovoltaics and organic semiconductor devices. This is due to its large bandgap of 3.5 eV, with the LUMO lying at a potential of 3.5 eV. However, when a silver layer is in contact with a bathocuproine layer in an organic diode, the formation of the silver-bathocuproine complex allows for efficient electron transport despite the large band gap.[33] This occurs due to the stabilization of the LUMO caused by the complex, which in an organic diode causes the LUMO of the bathocuproine layer to line up with the Fermi level of the silver layer, allowing for efficient electron transport.[34] In our sensor device, bathocuproine is adsorbed onto a p-type graphene surface through π-π stacking. As the bathocuproine adsorbs, the current through the FLG flake network decreases due to charge transfer occurring from the bathocuproine to the graphene layer. Holes are the primary charge carriers on FLG surfaces that have been exposed to ambient, and a decrease in hole density in the film will lead to a decrease in current. Once the sensor is exposed to Ag^+ ions, the positively charged complex that forms acts as an "electron trap", with charge transfer occurring from the graphene surface to the newly formed silver-bathocuproine complex. This increases the hole density in the film, which consequently increases the current.[35]

The formation of a silver-bathocuproine complex can be seen in the UV-Vis spectrum (Figure 3). As the silver (I) complexes, the peak at 286 nm experiences an increase in the absorbance, which indicates an increase in the transmission probability of the electrons after complexation due to the additional energy level between the HOMO (now the HOMO-1 of the complex) and the LUMO provided by the Ag^+ ion. Further evidence of complex formation comes from high resolution XPS data of the N 1s peak (Figure S1). While most nitrogen atoms in the pure bathocuproine powder have a 1s binding energy compatible with imines, the silver (I) complex shows an increase in the N 1s binding energy, similar to an amine or amide (the nitrate and nitrite peaks stem from the counter ions of the silver salt due

to the use of $AgNO_3$). In contrast, for bathocuproine molecules adsorbed onto FLG films as part of a sensor before and after exposure to 1 ppm of Ag^+ ions, there is no such shift in binding energy, as the binding energy of N 1s in the adsorbed bathocuproine already resembles an amine (Figure S2). Any electronic changes of the molecule during complex formation are directly handed through to the substrate. While Ag^+ ions struggle to interact with the non-functionalized sensor, as evidenced by a very small Ag 3d XPS peak (left side of Figure S3) and a low Ag / N atomic ratio (Table 1), they readily interact with bathocuproine-functionalized FLG films (right side of Figure S3). The silver in the adsorbed bathocuproine complex has an Auger parameter compatible with silver (0), meaning that it acted as an electron acceptor, or p-dopant as described above. This charge transfer between the graphene film and the silver-bathocuproine complex drives the response of the sensor.

3.2. Silver sensing and sensor optimization

The increase in hole density as Ag^+ ions bind to bathocuproine allows for quantification of Ag^+ ions in aqueous media. The concentration of Ag^+ ions in solution correlates with an increase in current through the sensor over a tested range of 3 ppb to 1 ppm, as seen during calibration of the sensor (Figure 4). Each increase in concentration gave a step up in current, which can be correlated to the concentration of Ag^+ ions in solution. This agrees with the behaviour predicted by the charge transfer mechanism between the graphene and bathocuproine once complexed to silver (I). This behaviour is highly reproducible across multiple functionalized devices (Figure S4), while unfunctionalized ("blank") sensor devices do not show any reliable or reproducible response over the tested Ag^+ ion concentration range. Furthermore, blank sensors tend to show visible signs of metallic silver deposition even at low silver concentrations (glittery appearance, Figure S5, right side) resulting in significant noise (Figure S4) on the sensor signal, while functionalized sensors can be used repeatedly without noise or signs of silver deposition (Figure S5, left side).

To ensure that optimal sensor performance is achieved, the functionalization of the sensors was optimized. Bathocuproine is known to dimerize in solution. The occurrence of a dimer or trimer occurs when the sp^2 hybridized imino groups of one bathocuproine monomer bond to the out-of-plane phenyl group of another monomer. This removes one active binding site (the silver (I) binds to the imine nitrogens in the molecule) and causes aggregates of the bathocuproine to clump up onto the FLG film, affecting further adsorption of other

bathocuproine monomers and detection of Ag^+ ions.[36] In concentrated solutions of bathocuproine, these aggregates can form heterogeneous multilayers on the graphene surface rather than a uniform self-assembled monolayer. The solution concentration will affect whether the bathocuproine molecules prefer to interact with each other in solution or with the graphene surface, so this parameter must be accounted for.[37,38] With this in mind, eight different sensors were evaluated, four with methanol and four with acetonitrile. The bathocuproine solution saturations for each solvent were 100%, 20%, 4%, and 0.8% relative to a fully saturated solution in the respective solvent. Sensors were exposed to the different bathocuproine solutions for 3 hours, and sensor performance was then analyzed in water by adding calculated amounts of Ag^+ aqueous stock solution to ultra pure water (Figure S6).

The sensors fabricated using 4% solutions had the largest and most reliable responses relative to the 0 ppm baseline over the widest Ag^+ concentration range for both methanol and acetonitrile. Acetonitrile was chosen as a solvent because it causes lesser swelling of the PDMS used as a dielectric protective layer than methanol.[39] Therefore, all subsequent devices used to characterize sensor performance (including Figure 3 and XPS data) were functionalized using a 4% (relative to fully saturated) bathocuproine solution in acetonitrile.

3.3. pH and conductivity response

Since the bathocuproine molecule has two imino groups, protonation will occur at low pH due to the presence of a lone pair on each of the nitrogen atoms. Based on the pK_a of neocuproine (5.79), it can be anticipated that the Ag^+ ion sensor would behave as a "proton sensor" below a pH of 6.[40] To confirm this, the response of the sensor to various pH was assessed to determine the optimal working range of the sensors. The responses were averaged between the four functionalized sensors and the two blank sensors. The error bars represent the standard deviation between replicates (Figure 5a).

From pH 10 to 6, there was no significant change in sensor response, indicating that it was stable over that range. However, once the pH changed from 6 to 5, a response of 24% (relative to the 0 ppm baseline) was seen, with the response increasing to 28% at pH 4, and 31% at pH 3. Based on these findings, the working range of this sensor is established to be from pH 6 to pH 10. Below pH 6 the bathocuproine adsorbed onto the FLG begins to protonate, while silver (I) hydroxide will start precipitating above pH 10. The sensor responses in Figure 3 are given relative to a baseline of purified water in the absence of added

ionic species. After addition of dilute NaOH to adjust the pH to 10, the ionic strength of the solution is significantly increased, further increasing as HNO_3 is added to reduce the pH. The resulting increase in conductance of the solution is the cause for the observed reduction in sensor film conductivity.

The conductance of the aqueous sample has to be taken into consideration because the ionic strength of the solution impacts the electrochemical double layer that is formed at surfaces in contact with it, including the surface of the chemiresistive sensors. A higher ionic strength would lead to a more compact double layer, leading to electrostatic gating of the resistive film.[41] Depending on the doping state and surface structure of the film, this may increase or decrease its resistance. A different impact on the sensors is also possible, if part of the current through the sensor was able to bypass it and flow through the analyte solution, thus adding a parallel resistance (potentially even lower than the original film) and thus leading to a marked decrease in resistance (i.e. increase in sensor current). The sensor response was thus tested as a function of conductivity by gradual addition of sodium bicarbonate to increase the ionic strength of the aqueous solution in the absence of Ag^+. The current response is shown to decrease with increasing conductance (Figure 5b), thus ruling out the possibility of a short circuit of the sensor current through the solution. This is consistent with our previous reports that short circuits though a conductive aqueous solution can be avoided by applying a sufficiently low voltage bias across the chemiresistive film.[19] An electrostatic gating effect from a more compact electrochemical double layer is confirmed, although smaller than the analyte response and opposite in sign. The ionic strength or conductivity of the analyte solutions will have to be taken into account when the sensor is calibrated, but since the response quickly saturates, this should not be an issue in practice.

3.4. Sensor reset and reuse

The reliance of this sensor on complexation of bathocuproine to Ag^+ ions makes its response time dependent on the time required to establish the binding equilibrium. At pH values higher than the pK_a of bathocuproine, the rate of dissociation of the silver-bathocuproine complex is much too slow, making a return to the baseline current quite time consuming. To rectify this, the sensor was reset back to the baseline using an acidic solution. Reducing the pH of the solution to less than 5.8 should drive equilibrium toward protonation of the imine groups in the ring structure and away from complexation toward Ag^+ ions. To reset the sensor, a pH 3

solution of HNO_3 was used (nitric acid was used to prevent precipitating silver (I) salts from solution by the anions associated with other acids) (Figure 6a). The sensors were kept in the pH 3 solution for one hour to allow for sufficient time to reset. While there was some baseline drift during the first cycle of the sensor (Figure S7), after the initial reset the baseline had stabilized at ~355 nA, returning to the same value after the two subsequent resets. This behaviour was reproducible in multiple devices (Figure S7). The percent changes post-reset also remained quite similar to their previous values, which show that this sensor can be reset and reused multiple times. Resetting can also be done in a reagent-less fashion through amperometric pH regulation. This method would be most useful for remote, online monitoring of water systems.[42-45]

XPS analysis was also performed on bare and bathocurpoine-functionalized FLG sensor films at three different stages of the sensing process: (1) after functionalization (or equivalent exposure to pure acetonitrile) and overnight exposure to water; (2) after subsequent exposure to 1 ppm of Ag^+ ions and (3) after subsequent resetting for 1 hour at pH 3. The Ag / N atomic ratio determined from the normalized Ag 3d and N 1s peaks in the survey spectra (Table 1) shows that the functionalized sensors adsorb significantly more silver upon exposure. Furthermore, the adsorption onto the sensor is almost completely reversible for the functionalized sensors only. The small residual amount of silver on the functionalized sensors after reset at pH 3 for 1 hour is likely correlated to defects in the sensing film and explains the observation that the first reset of any new device is incomplete, unlike those of subsequent cycles (Figure S7). It nevertheless does not appear to impede further function of the device.

3.5. Analytical performance

The changes in current relative to the baseline can be correlated to the concentration of Ag^+ ions in solution. This correlation can take the form of a function that can be used to interpolate or extrapolate the concentration with any given change in current. Based on the underlying mechanism two functions can be considered for this calibration curve, namely the Langmuir isotherm and a first-order reaction function (exponential). The Langmuir isotherm assumes that the adsorbate (in our case the complexation of Ag^+) binds to distinct and independent sites (1), and that the sensor response is directly related to the concentration of bound species.

$$\theta_A = \theta_{A,m} \frac{K^A_{eq}[A]}{1+K^A_{eq}[A]} \quad (1)$$

In this function, θ_A is the occupancy of sites, $\theta_{A,m}$ is the saturation point, K is the equilibrium constant (corrected for the sensor response function), and [A] is the concentration of the adsorbate. Since Ag^+ ions form a 1:1 complex with bathocuproine, this would be a fair assumption.[46] Alternatively, the formation of a 1:1 complex can also be modelled by a first-order type exponential decay fit (2).

$$\theta_A = \theta_{A,m}(1 - e^{-k[A]}) \quad (2)$$

In this function, θ_A is the product formed, $\theta_{A,m}$ is the maximum amount of product that can be formed, and k is the rate constant.[47] In this empirical relationship the assumptions of coverage being limited to a monolayer and proportional sensor response are removed, but the inclusion of (0, 0) in the calibration curve as well as the asymptotic behaviour (saturation) of the sensor response at high concentration are maintained. The average relative current changes of the same sensor between reset cycles were plotted (blue dots) and a Langmuir and exponential fit were plotted together with it (Figure 6b).

The Langmuir curve gave constant values of 30.87% for $\theta_{A,m}$ and 0.0033 M^{-1} for K^A_{eq}, with an R^2 of 0.9982. The first order exponential decay curve gave constant values of 24.45% for $\theta_{A,m}$ and a value of 0.0034 $M^{-1}s^{-1}$ for k, with an R^2 value of 0.9939. The Langmuir fit indicates that the sensor will saturate at a relative current of 30.87%, with 1 ppm of Ag^+ resulting in a current change of 23.92±1.05%. The exponential model has an even lower saturation current change of 24.45%, which would indicate that the sensor response will saturate beyond 1 ppm for the Ag^+ ion sensor. The current changes were reproducible, with the values having a standard deviation no greater than 1.24% over the three reset-step up cycles. The limit of detection - calculated using an s/σ ratio of 3 - was determined to be 3 ppb. The response of the sensor was also linearized by plotting the concentration of Ag^+ against the ratio of the Ag^+ concentration to the current response, and was found to have a linear range of 30 ppb to 1 ppm (Figure S8).

As the concentration exceeded 1 ppm, reduction of Ag^+ to elemental Ag occurred due to the flow of current in the FLG film. This was evident from large noise in the sensor response (Figure S6), as well as a glittery appearance of the exposed sensors similar to the non-functionalized sensor shown in Figure S5. Thus, the effective maximum measurable concentration for this sensor is 1 ppm.

3.6. Interferences

The sensors were tested against a range of common interfering ions to determine feasibility for use in environmental and industrial settings (Figure 7a). The following interferant concentrations were used, based on common concentrations in real samples [32]: Cr^{3+} (0.1 ppm), Co^{2+} (1 ppm), Al^{3+} (1 ppm), Cd^{2+} (0.1 ppm), SO_4^{2-} (250 ppm), Fe^{2+} (1 ppm), Cl^- (100 ppm), PO_4^{3-} (1 ppm), NO_3^- (50 ppm), K^+ (1 ppm), Zn^{2+} (1 ppm), Cu^{2+} (1 ppm), Mg^{2+} (1 ppm), Ca^{2+} (10 ppm). Each interferant was tested individually in the given order, with sensors being reset and rinsed between interferants. At the end, the sensor response to 100 ppb of Ag^+ ions was also tested. All devices thus underwent 11 sensing and reset cycles over 15 hours for the purpose of this experiment (in addition to overnight rest periods in water), showing no signs of degradation and fully responding to Ag^+ ions at the end. No significant interference was found from the interferants at the tested concentrations, with the exception of Cu^{2+}, which at 1 ppm was shown to give almost half of the response of 100 ppb of Ag^+ ions. Copper is directly above silver on the periodic table. Due to their chemical similarity it does not surprise that copper would interfere with the silver (I) sensor response. However, it has a preference for an oxidation state of +2, whereas bathocuproine only binds to metals with a d^{10} electron configuration and a +1 oxidation state, making the sensors more selective toward silver (I) in an oxidizing environment (presence of dissolved oxygen). In environmental water samples, Cu^{2+} is also very sparse, with concentrations rarely exceeding the low-ppb levels.[32] In situations where Cu^{2+} interference is of concern, use of a sensing array would be most appropriate in order to retain reagent-free operation as one of the main advantages of these sensors. Since these sensors are very simple and robust, a bathocuproine sensor may be paired with a sensor more selective to Cu^{2+}, e.g. by modifying the FLG film with neocuproine, which is known to complex with Cu^{2+}.[48] This sensor can be used concurrently with the Ag^+ sensor to determine both Cu^{2+} and Ag^+ simultaneously. Sensors tested with neocuproine show a good response for Cu^{2+} with negligible interference from Ag^+ (Figures S9, S10). Although further characterization is required, the neocuproine functionalized sensor is a potential solution to the interference from Cu^{2+}.

3.7. Real sample analysis

Real sample analysis was conducted using water collected from Spencer creek, a water source in the Dundas area in Hamilton, Ontario. A calibration curve was prepared prior to testing the real water sample by using ultrapure (18.2 MΩ·cm) water with added sodium bicarbonate and nitric acid to adjust its conductance and pH to approximate those of the river water sample (actual river sample values were measured to be 203 μS/cm and pH 8.7). In contrast, the calibration curve shown in Figure 4 was taken in ultrapure water and did not have its pH and conductivity adjusted to any specific sample. A portion of the real water sample was acidified with nitric acid [49] and sent for testing for Ag^+ ions using ICP-MS as the laboratory standard method for metal ion analysis, in addition to sample aliquots that were spiked with additional 20 ppb, 50 ppb or 80 ppb of Ag^+ (Table 2, full analysis report in the Supporting Material). The chemiresistive sensors were able to detect Ag^+ ions in all of the spiked samples, with recovery values of 108.8±4.4%, 106.8±13.9%, and 98.7±2.4% for the 20 ppb, 50 ppb or 80 ppb spiked samples respectively. The responses from the real sample were interpolated from the calibration curve. While 20 ppb was outside the linear range (30 ppb to 1 ppm) of the chemiresistive sensor, an approximte value (albeit with higher error) could still be obtained from the Langmuir-style calibration function.

To test the potential impact of anions on the sensor response, the devices were exposed to increasing amounts of nitrate while the concentration of Ag^+ ions remained constant at 100 ppb (Figure 7b). From this test, it is apparent that the sensor current decreases with increasing amounts of nitrate. In our real sample, nitrate was present at a concentration of 790 ppb (Table 3), which would result in a response reduction of about 2%. Matrix effects due to the presence of other ions do therefore need to be taken into account. Alternatively, a nitrate sensors might be able to be developed based on the Ag-bathocuproine complex, although the overall response is rather small. Another interesting observation from the nitrate interference experiment results in Figure 7b is that the sensor responses were much faster than for Ag^+ ions. The shorter time constant is consistent with an electrostatic gating mechanism from the negatively charged nitrate ions accumulating near the sensor surface. This is similar to the conductivity response in Figure 5, but much higher in magnitude. The higher magnitude of the current results from preferential interactions of the nitrate ions with the bathocuproine-silver (I) complex. Nitrate is always present in all our experiments as a counter ion to Ag^+, but now its concentration is significantly increased. Furthermore, the distinction between the electrostatic gating and charge transfer doping mechanisms is highlighted by the differing (in speed and sign) responses of our devices.[20]

4. Conclusion

A chemiresistive sensor was demonstrated for the detection of aqueous Ag^+ ions. Due to the phenanthroline backbone of the bathocuproine, it could be stably adsorbed onto a percolation network of exfoliated FLG flakes forming a chemiresistive film. The binding of bathocuproine to Ag^+ ions was confirmed by UV-Vis spectroscopy. The sensors were calibrated over a range from 3 ppb to 1 ppm, fitting to both a Langmuir isotherm and a first-order exponential decay function, providing R^2 values of 0.9982 and 0.9939 respectively. Interference studies demonstrated strong selectivity for Ag^+ ions over other cations commonly found in surface waters. The limit of detection (LOD) for this sensor calculated using the s/σ ratio is 3 ppb, and the detection range goes from 30 ppb to 1 ppm (Table 4). The sensors can detect Ag^+ ions in an approximate pH range of 10 to 6 but will not respond to particulate silver species. Sensors can be reset by exposure to low pH and reused, thus enabling continuous online monitoring applications. Sensors response is somewhat sensitive to pH and ionic strength of the sample, thus requiring pH control and calibration to an approximate range of anticipated ionic strength. For commercial applications, the sensor fabrication method will have to be refined to reduce the heterogeneity of the FLG film and improve the uniformity of the bathocuproine coating on the FLG film. At present each sensor requires its own unique calibration curve, rather than one universal curve for an entire batch of sensors. While we assume the formation of a self-assembled monolayer (SAM) of bathocuproine[50], we do not know the details of its structure (e.g. orientation of the molecules) or uniformity, which should be subject to a more fundamental study of these systems. Nevertheless, the development of this sensor platform opens up a new pathway toward aqueous metal cation sensing, and through modification of the adsorbate can be used to detect many other analytes. Deployment of these sensors for real life monitoring applications will in fact require the development of sensing arrays capable of multiple ion detection. As a first step, we have demonstrated that neocuproine (a closely related molecule to bathocuproine) can be used to detect Cu^{2+}, such that Ag^+ and Cu^{2+} could be quantified simultaneously.

Supplementary material

See supplementary material for additional and replicate sensing data, XPS spectra and real water sample analysis by ICP-MS and ion chromatography.

Johnson Dalmieda: Methodology, Investigation, Writing - Original Draft

Ana Zubiarrain-Laserna: Methodology, Investigation, Writing - Original Draft

Devanjith Ganepola: Investigation

P. Ravi Selvaganapathy: Conceptualization, Writing - Review & Editing

Peter Kruse: Supervision, Conceptualization, Methodology, Writing - Review & Editing

Declaration of interests

The authors declare that they have no known competing financial interests or personal relationships that could have appeared to influence the work reported in this paper

Acknowledgements

The authors thank David J. H. Emslie for fruitful discussions, as well as Dipankar Saha, Arjun Rego, and Jonah Halili for their support. The authors are indebted to Dr. Mark Biesinger at Surface Science Western for assistance with XPS. Electron microscopy was performed at the Canadian Centre for Electron Microscopy (also supported by NSERC and other government agencies). The authors thank Activation Laboratories Ancaster for analyzing the rain water runoff sample. The authors also acknowledge financial support from the Natural Sciences and Engineering Research Council of Canada through the Discovery Grant Program (award number RGPIN06145-18), as well as the Canada First Research Excellence Fund project “Global Water Futures”.

References

[1] J. S. Kim, E. Kuk, K. N. Yu, J.-H. Kim, S. J. Park, H. J. Lee, S. H. Kim, Y. K. Park, Y. H. Park, C.-Y. Hwang, et al. Antimicrobial Effects of Silver Nanoparticles, Nanomed. Nanotechnol., Biol. Med. 3 (2007) 95–101.

[2] S. Triantafyllidou, D. Lytle, C. Muhlen, J. Swertfeger, Copper-silver ionization at a US hospital: Interaction of treated drinking water with plumbing materials, aesthetics and other considerations, Water Res. 102 (2016) 1-10.

[3] J. P. Marshall, Systemic Argyria Secondary to Topical Silver Nitrate, Arch. Dermatol. 113 (1977) 1077.

[4] G. D. DiVincenzo, C. J. Giordano, L. S. Schriever, Biologic Monitoring of Workers Exposed to Silver, Int. Arch. Occup. Environ. Health 56 (1985) 207–215.

[5] Agency for Toxic Substances and Disease Registry, Toxicological Profile for Silver, 1990.

[6] O. Bondarenko, K. Juganson, A. Ivask, K. Kasemets, M. Mortimer, A. Kahru, Toxicity of Ag, CuO and ZnO Nanoparticles to Selected Environmentally Relevant Test Organisms and Mammalian Cells in Vitro: A Critical Review, Arch. Toxicol. 87 (2013) 1181–1200.

[7] World Health Organization, Silver as a Drinking-Water Disinfectant, 2018.

[8] S. Lee, K. Jang, C. Park, J. You, T. Kim, C. Im, J. Kang, H. Shin, C.-H. Choi, J. Park, et al. Ultra-Sensitive in Situ Detection of Silver Ions Using a Quartz Crystal Microbalance, New J. Chem. 39 (2015) 8028–8034.

[9] C. Qin, W.-Y. Wong, L. Wang, A Water-Soluble Organometallic Conjugated Polyelectrolyte for the Direct Colorimetric Detection of Silver Ion in Aqueous Media with High Selectivity and Sensitivity, Macromol. 44 (2011) 483–489.

[10] C.-Y. Lin, C.-J. Yu, Y.-H. Lin, W.-L. Tseng, Colorimetric Sensing of Silver (I) and Mercury (II) Ions Based on an Assembly of Tween 20-Stabilized Gold Nanoparticles, Anal. Chem. 82 (2010) 6830–6837.

[11] A. Chatterjee, M. Santra, N. Won, S. Kim, J. K. Kim, S. B. Kim, K. H. Ahn, Selective Fluorogenic and Chromogenic Probe for Detection of Silver Ions and Silver Nanoparticles in Aqueous Media, J. Am. Chem. Soc. 131 (2009) 2040–2041.

[12] M. Chae, A. Czarnik, Fluorometric Chemodosimetry. Mercury (II) and Silver (I) Indication in Water Via Enhanced Fluorescence Signaling, J. Am. Chem. Soc. 114 (1992) 9704–9705.

[13] N. Rubinova, K. Chumbimunitorres, E. Bakker, Solid-Contact Potentiometric Polymer Membrane Microelectrodes for the Detection of Silver Ions at the Femtomole Level, Sens. Actuators B Chem. 121 (2007) 135–141.

[14] K. O'Connor, G. Svehla, S. Harris, M. McKervey, Calixarene-Based Potentiometric Ion-Selective Electrodes for Silver, Talanta 39 (1992) 1549–1554.

[15] D. Schildkraut, P. Dao, J. Twist, A. Davis, K. Robillard, Determination of Silver Ions At Submicrogram-Per-Liter Levels Using Anodic Square-Wave Stripping Voltammetry, Environ. Toxicol. Chem. 17 (1998) 642–649.

[16] H. Zejli, J. Cisneros, I. Naranjo-Rodriguez, K. Temsamani, Stripping Voltammetry of Silver Ions At Polythiophene-Modified Platinum Electrodes, Talanta 71 (2007) 1594–1598.

[17] P. Kruse, Review on Water Quality Sensors, J. Phys. D 51 (2018) 203002.

[18] J. Dalmieda, P. Kruse, Metal Cation Detection in Drinking Water, Sensors 19 (2019) 5134.

[19] A. Mohtasebi, P. Kruse, Chemical Sensors Based on Surface Charge Transfer, Phys. Sci. Rev. 3 (2018) 20170133.

[20] A. Zubiarrain-Laserna, P. Kruse, Graphene-Based Water Quality Sensors, J. Electrochem. Soc. 167 (2020) 037539.

[21] Geim, A. K. Graphene: Status and Prospects. Science 2009, 324 (5934), 1530–1534.

[22] E. Hoque, T. Chowdhury, P. Kruse, Chemical in Situ Modulation of Doping Interactions between Oligoanilines and Nanocarbon Films, Surf. Sci. 676 (2018) 61–70.

[23] T. Saito, Transport of Silver(I) Ion through a Supported Liquid Membrane Using Bathocuproine as a Carrier, Sep. Sci. Technol. 33 (1998) 855–866.

[24] A. Mohtasebi, A. D. Broomfield, T. Chowdhury, P. R. Selvaganapathy, P. Kruse, Reagent-Free Quantification of Aqueous Free Chlorine via Electrical Readout of Colorimetrically Functionalized Pencil Lines, ACS Appl. Mater. Interfaces 9 (2017) 20748–20761.

[25] E. Hoque, L. H.-H. Hsu, A. Aryasomayajula, P. R. Selvaganapathy, P. Kruse, Pencil-Drawn Chemiresistive Sensor for Free Chlorine in Water, IEEE Sens. Lett. 1 (2017) 4500504.

[26] L. H.-H. Hsu, E. Hoque, P. Kruse, P. R. Selvaganapathy, A Carbon Nanotube Based Resettable Sensor for Measuring Free Chlorine in Drinking Water, Appl. Phys. Lett. 106 (2015) 063102.

[27] Gong, J.-L.; Sarkar, T.; Badhulika, S.; Mulchandani, A. Label-Free Chemiresistive Biosensor for Mercury (II) Based on Single-Walled Carbon Nanotubes and Structure-Switching DNA. Applied Physics Letters 2013, 102 (1), 013701.

[28] Moffett, J. W.; Zika, R. G.; Petasne, R. G. Evaluation of Bathocuproine for the Spectro-Photometric Determination of Copper(I) in Copper Redox Studies with Applications in Studies of Natural Waters. Analytica Chimica Acta 1985, 175, 171–179.

[29] U. Halim, C. R. Zheng, Y. Chen, Z. Lin, S. Jiang, R. Cheng, Y. Huang, X. Duan, A Rational Design of Cosolvent Exfoliation of Layered Materials by Directly Probing Liquid–Solid Interaction, Nat. Commun. 4 (2013) 2213. doi: 10.1038/ncomms3213.

[30] A. C. Ferrari, J. C. Meyer, V. Scardaci, C. Casiraghi, M. Lazzeri, F. Mauri, S. Piscanec, D. Jiang, K. S. Novoselov, S. Roth, A. K. Geim, Raman Spectrum of Graphene and Graphene Layers, Phys. Rev. Lett. 97 (2006) 187401.

[31] M. S. Dresselhaus, A. Jorio, A. G. Souza Filho, R. Saito, Defect characterization in graphene and carbon nanotubes using Raman spectroscopy, Philos. Trans. R. Soc. A Math. Phys. Eng. Sci. 368 (2010) 5355–5377.

[32] Government of Ontario, Provincial Water Quality Monitoring Network Website https://www.ontario.ca/environment-and-energy/map-provincial-stream-water-quality-monitoring-network (accessed 10 April 2020).

[33] B. R. Patil, M. Ahmadpour, G. Sherafatipour, T. Qamar, A. F. Fernández, K. Zojer, H.-G. Rubahn, M. Madsen, Area Dependent Behavior of Bathocuproine (BCP) as Cathode Interfacial Layers in Organic Photovoltaic Cells, Sci. Rep. 8 (2018) 12608. doi: 10.1038/s41598-018-30826-7.

[34] H. Yoshida, Electron Transport in Bathocuproine Interlayer in Organic Semiconductor Devices, J. Phys. Chem. C 119 (2015) 24459–24464.

[35] S. Mao, J. Chang, H. Pu, G. Lu, Q. He, H. Zhang, J. Chen, Two-Dimensional Nanomaterial-Based Field-Effect Transistors for Chemical and Biological Sensing, Chem. Soc. Rev. 46 (2017) 6872–6904.

[36] F. Shojaie, Theoretical Studies on Dimerization Reactions of 4, 7-Diphenyl-1,10-Phenanthroline (BPhen) and Bathocuproine (BCP) in Organic Semiconductors, Semiconductors 48 (2014) 1051–1062.

[37] D. K. Schwartz, Mechanisms and Kinetics of Self-Assembled Monolayer Formation, Annu. Rev. Phys. Chem. 52 (2001) 107–137.

[38] N. Rozlosnik, M. C. Gerstenberg, N. B. Larsen, Effect of Solvents and Concentration on the Formation of a Self-Assembled Monolayer of Octadecylsiloxane on Silicon (001), Langmuir 19 (2003) 1182–1188.

[39] J. N. Lee, C. Park, G. M. Whitesides, Solvent Compatibility of Poly(Dimethylsiloxane)-Based Microfluidic Devices, Anal. Chem. 75 (2003) 6544–6554.

[40] Z. Xiao, J. Brose, S. Schimo, S. M. Ackland, S. L. Fontaine, A. G. Wedd, Unification of the Copper(I) Binding Affinities of the Metallo-Chaperones Atx1, Atox1, and Related Proteins, J. Biol. Chem. 286 (2011) 11047–11055.

[41] I. Heller, S. Chatoor, J. Männik, M. A. G. Zevenbergen, C. Dekker, S. G. Lemay, Influence of Electrolyte Composition on Liquid-Gated Carbon Nanotube and Graphene Transistors, J. Am. Chem. Soc. 132 (2010) 17149–17156.

[42] L. T.-H. Kao, H.-Y. Hsu, M. Gratzl, Reagentless pH-Stat for Microliter Fluid Specimens, Anal. Chem. 80 (2008) 4065–4069.

[43] R. Hagedorn, J. Korlach, G. Fuhr, Amperometric pH Regulation - a Flexible Tool for Rapid and Precise Temporal Control over the pH of an Electrolyte Solution, Electrophoresis 19 (1998) 180–186.

[44] E. L. May, A. C. Hillier, Rapid and Reversible Generation of a Microscale pH Gradient Using Surface Electric Fields, Anal. Chem. 77 (2005) 6487–6493.

[45] K. Morimoto, M. Toya, J. Fukuda, H. Suzuki, Automatic Electrochemical Micro-pH-Stat for Biomicrosystems, Anal. Chem. 80 (2008) 905–914.

[46] D. A. H. Hanaor, M. Ghadiri, W. Chrzanowski, Y. Gan, Scalable Surface Area Characterization by Electrokinetic Analysis of Complex Anion Adsorption, Langmuir 30 (2014) 15143–15152.

[47] A. Leike, Demonstration of the Exponential Decay Law Using Beer Froth, Eur. J. Phys. 23 (2001) 21–26.

[48] Gouda, A. A.; Amin, A. S. Copper(II)–Neocuproine Reagent for Spectrophotometric Determination of Captopril in Pure Form and Pharmaceutical Formulations. Arabian Journal of Chemistry 2010, 3 (3), 159–165.

[49] USEPA, 1994. Method 200.8: Determination of Trace Elements in Waters and Wastes by Inductively Coupled Plasma - Mass Spectrometry, Revision 5.4. Environmental Monitoring Systems Laboratory, Office of Research and Deveopment, Cincinnati, OH.

[50] Barlow, S. M.; Raval, R. Complex Organic Molecules at Metal Surfaces: Bonding, Organisation and Chirality. Surface Science Reports. (2003) 201–341.

Johnson Dalmieda received his B.Sc. (Hons) in Chemistry from McMaster University in 2018, with his undergraduate thesis focusing on the Seebeck effect in molecular diodes. As an M.Sc. student, he is presently working on carbon-based chemiresistive sensors for the detection and quantification of metal cations in water, with a particular focus on the metal-ligand interaction between the metal cations and the selective ionophore used to functionalize the sensors.

Ana Zubiarrain-Laserna received her B.Sc. in Chemistry from the University of the Basque Country (Spain) in 2017 and her M.Sc. in Chemistry from McMaster University (Canada) in 2019. During her Masters degree she worked under the supervision of Professor Peter Kruse, developing nanocarbon-based chemiresistive water quality sensors. Her current research interests include materials science, green chemistry, and science communication.

Devanjith Ganepola is a recent graduate from McMaster University in 2020 where he received his B.Sc (Honours) in Chemical Biology. The scope of his undergraduate thesis involved functionalizing graphite-based chemiresistive sensors for nitrate ion detection in aqueous media. Pursuing his passion for chemistry and its application in a medical setting, he will be continuing as Masters candidate in the Medical Sciences Program at McMaster University where he will be adapting existing GC-MS methods to APGC-MS to determine inborn errors in metabolism of patients.

Dr. P. Ravi Selvaganapathy is a Professor of Mechanical and Biomedical Engineering at McMaster University and the Canada Research Chair in Biomicrofluidics. His research interests are in microfluidic devices for diagnostics, drug discovery, diagnostics and artificial organs. He has more than 20 years of extensive experience in micro/nano fabrication and microfluidics which has resulted in ~110 journal publications, 50 conference publications, 35 invited talks and 8 patents. His research has won several best paper awards and highlighted on journal covers. He won the Early Researchers Award in 2010 and has been named as a Rising Star in Global Health in 2012.

Dr. Peter Kruse obtained a Diploma in Chemistry in 1995 from Friedrich Schiller University, Jena, Germany and a PhD in Chemistry in 2000 from the University of California, San Diego.

After a postdoctoral fellowship at the National Research Council of Canada he joined the Department of Chemistry and Chemical Biology at McMaster University in Hamilton, Ontario (Canada). Surface science research in the Kruse group over the last 18 years has spanned chemical doping of carbon nanotubes, corrosion inhibition on steel, mobility at interfaces, anodic pattern formation in electrochemistry, 2D materials and chemiresistive sensors.

Figure Captions

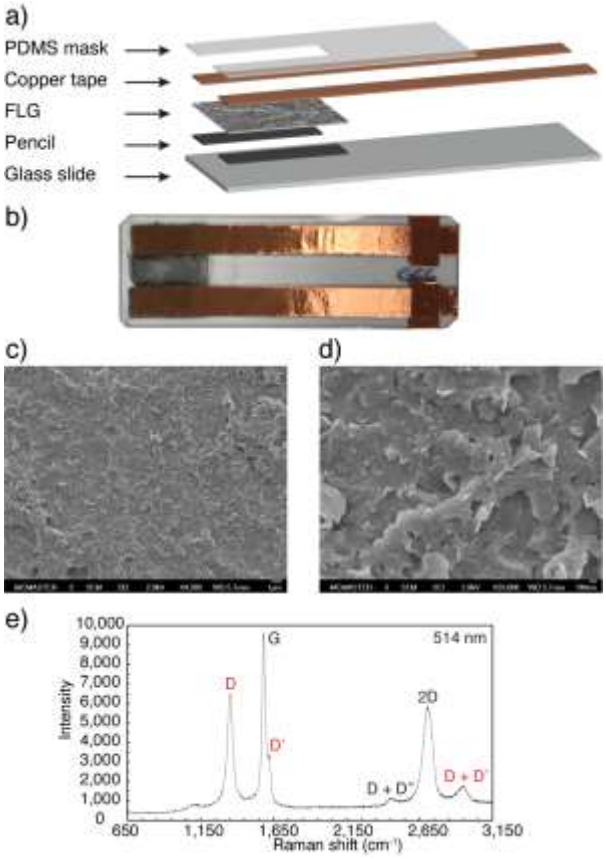

Figure 1. a) Components of a sensor. **b)** Picture of a finished sensor. **c – d)** FESEM images of the few layer graphene (FLG) film at different magnifications: **c)** × 4,300 and **d)** × 33,000. **e)** Raman spectrum of the FLG film. The peaks labelled in black are characteristic of FLG, while the peaks labelled in red indicate the presence of defects.

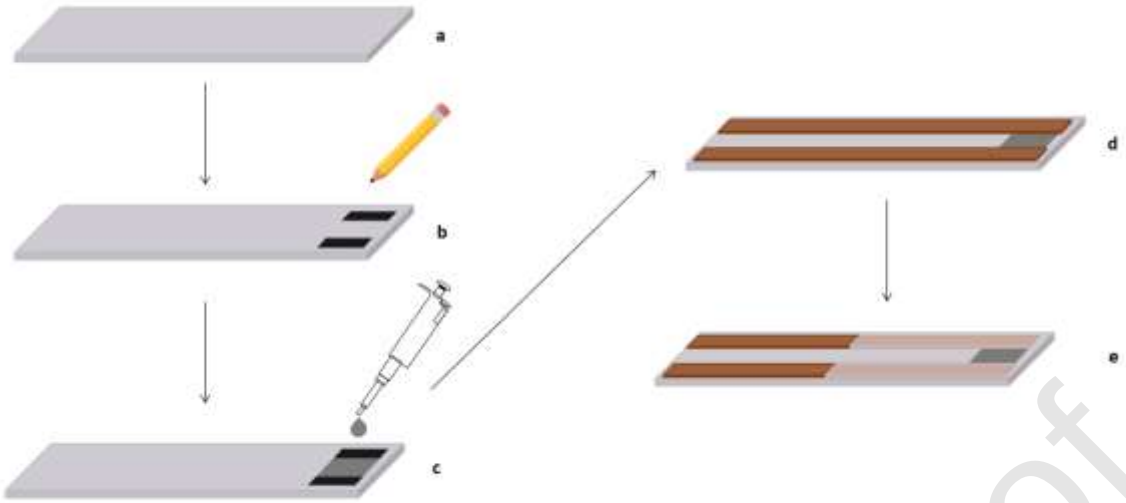

Figure 2. Detailed instructions for the fabrication of the chemiresistive sensor. **a)** Prepare and clean a twin-frosted glass slide. **b)** Draw two thick pencil pads on either end of the glass slide using a 9B pencil. **c)** Drop cast the exfoliated graphite between the pencil pads at 100°C. **d)** Apply conductive copper tape lengthwise along the sensor overlapping the pencil pads. **e)** Apply PDMS over the copper tape at 60°C and allow to cure.

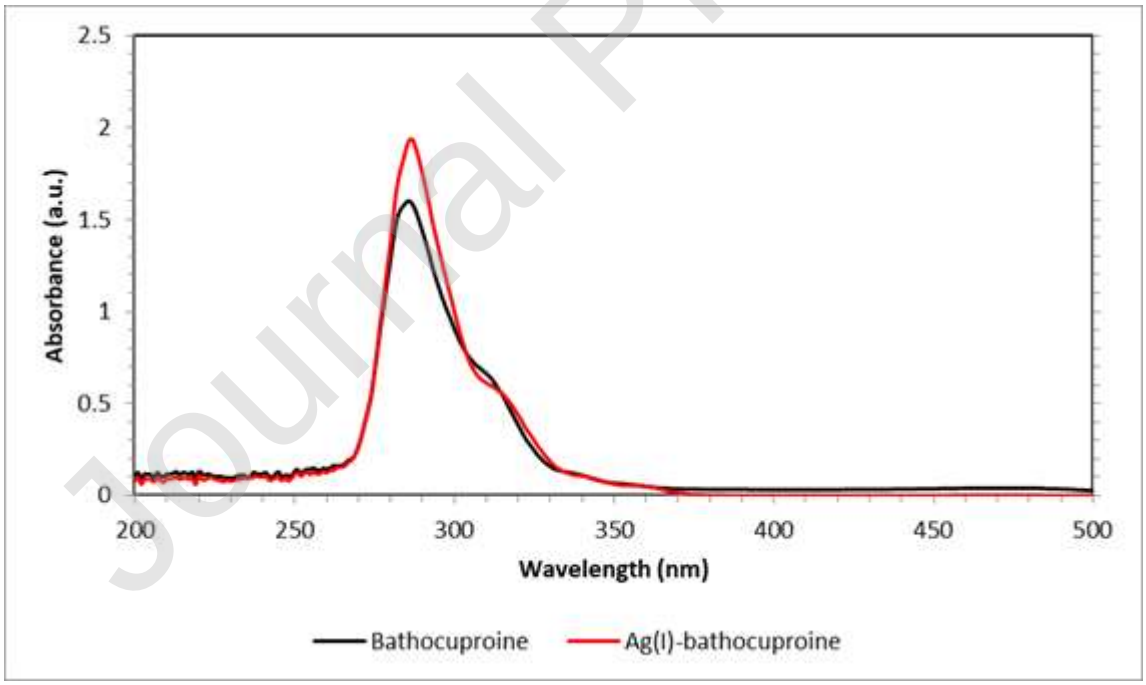

Figure 3. UV-Vis spectra of bathocuproine (black) and the silver (I)-bathocuproine complex (red). Inset: Structure of bathocuproine. The complex with silver will be formed by interaction with the two nitrogen atoms.

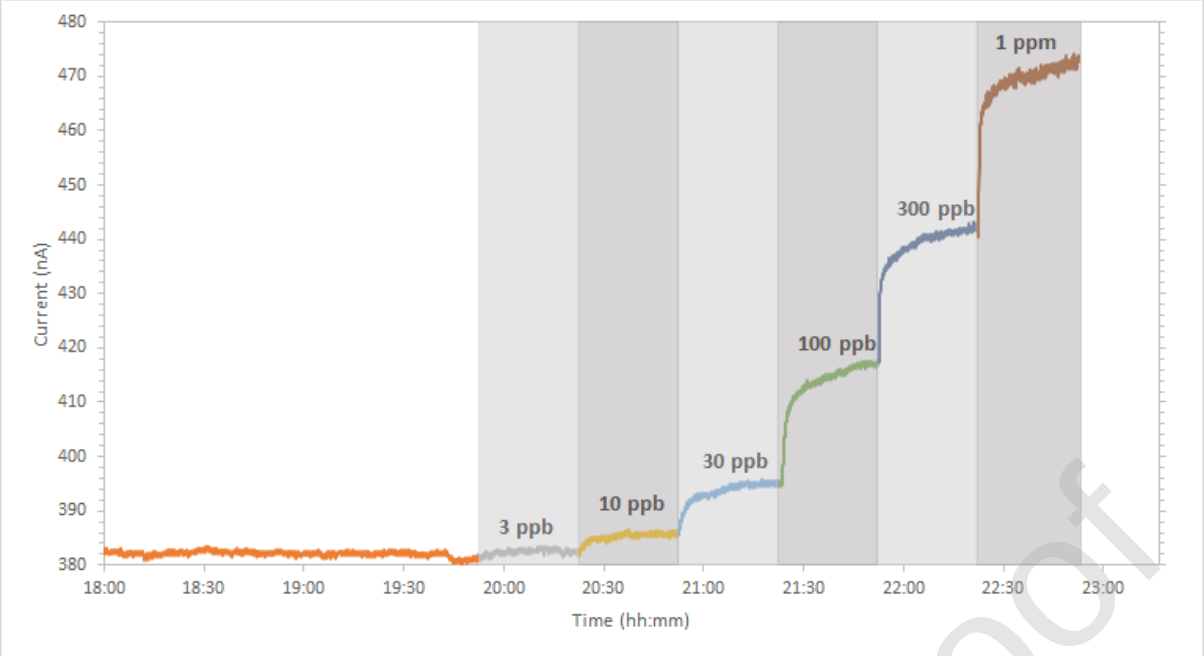

Figure 4. Current response to different concentrations of silver (I) in solution. Concentrations below 30 ppb took ~15 minutes to reach a stable current value. Above this, stabilization only took ~5 minutes.

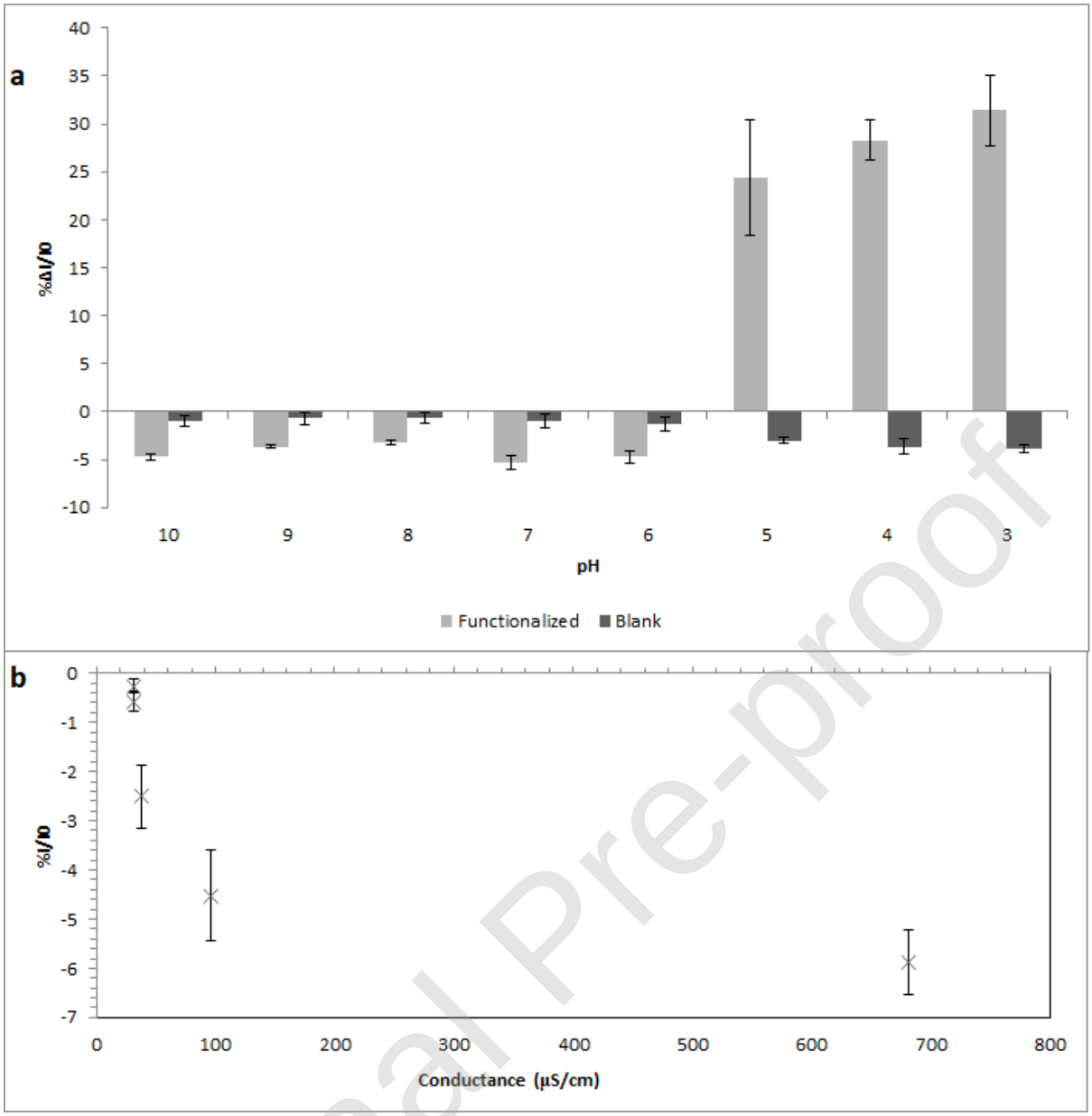

Figure 5. a) Comparison of the sensor response to changes in pH. Only the bathocuproine functionalized sensors exhibit a change in response direction from decreasing to increasing, confirming that functionalization has occurred and that a pH reset is possible. **b)** Sensor response due to conductivity of the aqueous solution. A response in the opposite direction of the silver (I) response indicates the presence of an electrostatic gating effect in the presence of high-conductance aqueous samples.

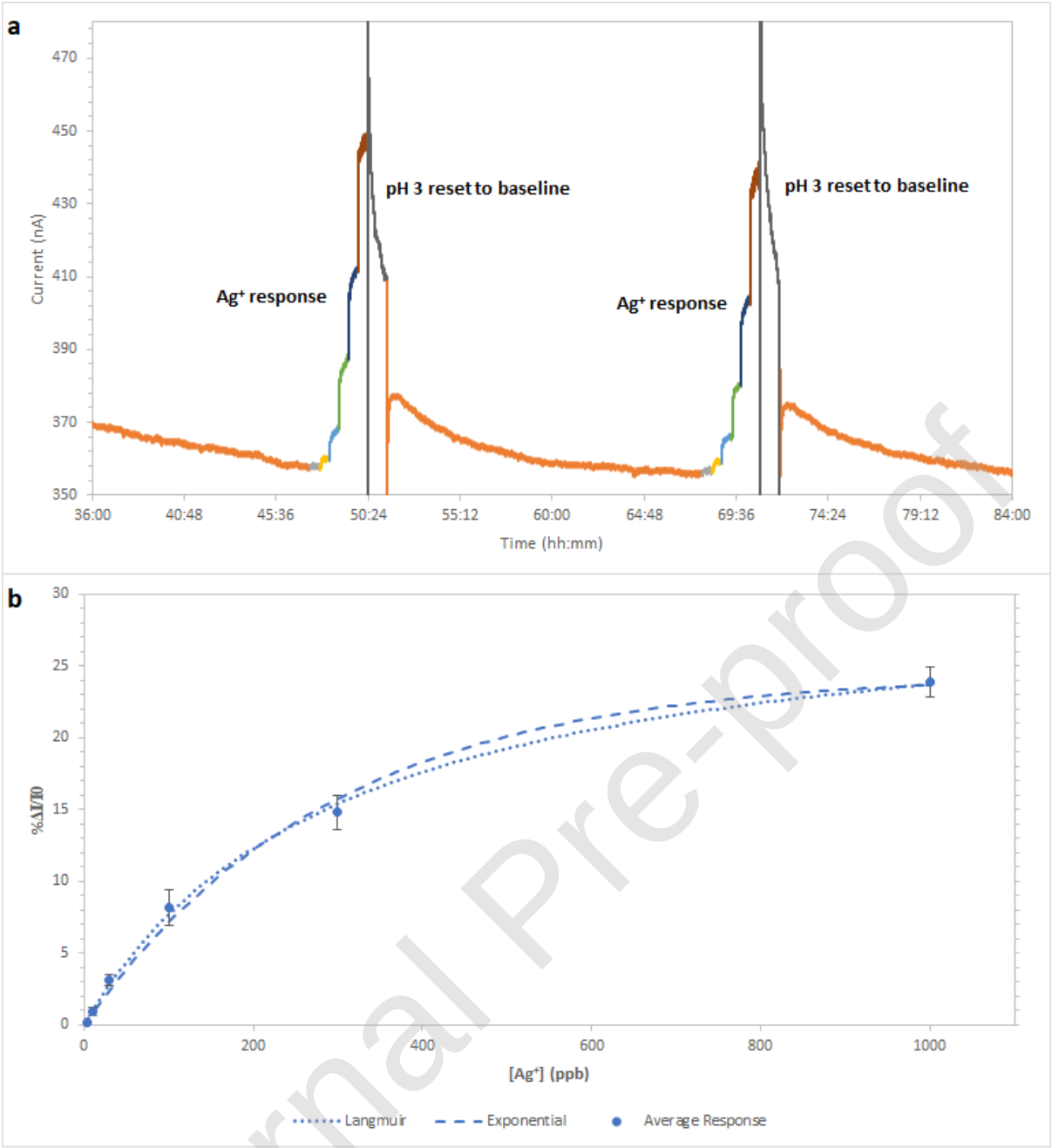

Figure 6. a) Sensor reset with pH 3 HNO_3. It takes 1 hour for the sensor to reach the previous baseline, after which silver (I) can be spiked into solution once again. **b)** Average relative change in current, with the Langmuir and exponential decay function plotted alongside.

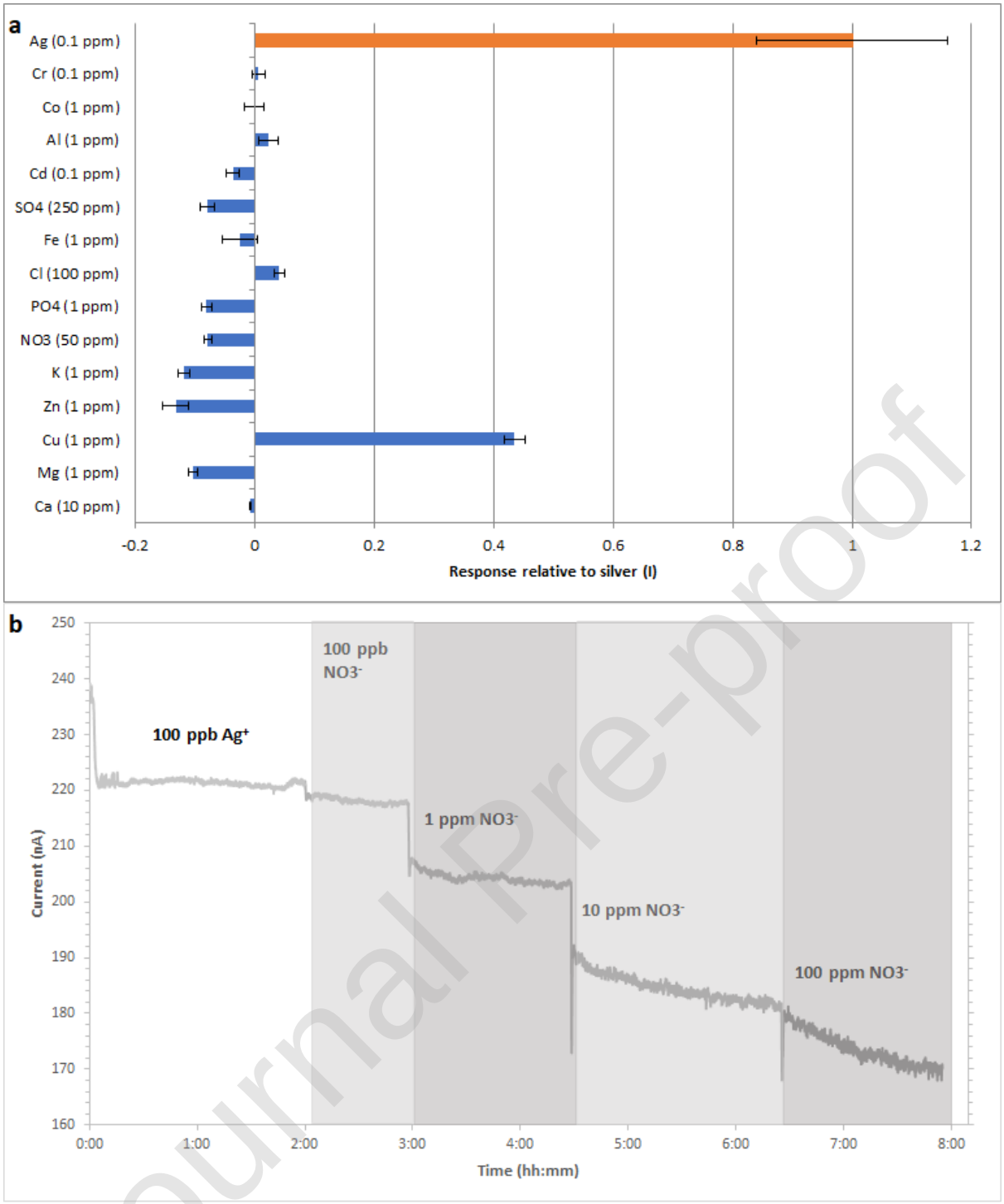

Figure 7. a) Interferences with their relative responses compared to silver (I). The interferences were run in a bicarbonate/nitrate background, with a conductance value of 31 µS/cm and a pH of 6.7. **b)** Current response to different concentrations of nitrate in solution with a constant background of 100 ppb silver (I).

Tables

Table 1. Sample composition based on XPS survey spectra (Ag 3d, N 1s) of bathocuproine and silver-bathocuproine complex powder samples as well as non-functionalized and functionalized sensors preserved at different stages of the sensing procedure. The Ag / N ratio was calculated from atomic% values.

Sample	Ag / N atomic ratio
Non-functionalized sensor	0.00
Non-functionalized sensor + 1 ppm Ag^+	0.30
Non-functionalized sensor + 1 ppm Ag^+ + pH 3 HNO_3 reset	0.17
Functionalized sensor	0.00
Functionalized sensor + 1 ppm Ag^+	1.40
Functionalized sensor + 1 ppm Ag^+ + pH 3 HNO_3 reset	0.25

Table 2. Real sample and spike tests for the silver (I) sensor.

Added (ppb)	Found by sensor (ppb)	Found by ICP-MS (ppb)	Recovery (%)
0	<3.0	<0.2	-
20	21.8±0.9	23.7	108.8±4.4%
50	53.4±6.9	45.2	106.8±13.9%
80	79.0±1.9	81.0	98.7±2.4%

Table 3. Ion chromatography results for the real sample.

Anion	Amount (ppm)
F^-	0.12
Cl^-	103
NO_3^-	0.79
SO_4^{2-}	64.1
PO_4^{3-}	<0.1

Table 4. Our method of silver (I) detection compared with other methods.

Method	LOD (ppm)	Linear Range (ppm)	Reference
Fluorescent/Colorimetric	0.014	0.014-0.539	[11]
Potentiometric	10	17-1710	[14]
Anodic Stripping Voltammetry	0.060	0.070-1	[16]
Chemiresistive	0.003	0.030-1	This work